nature COMMUNICATIONS

18 Feb, 2021

Structural characterization of ice XIX as the second polymorph related to ice VI

Tobias M. Gasser [1], Alexander V. Thoeny [1], A. Dominic Fortes [2] & Thomas Loerting [1✉]

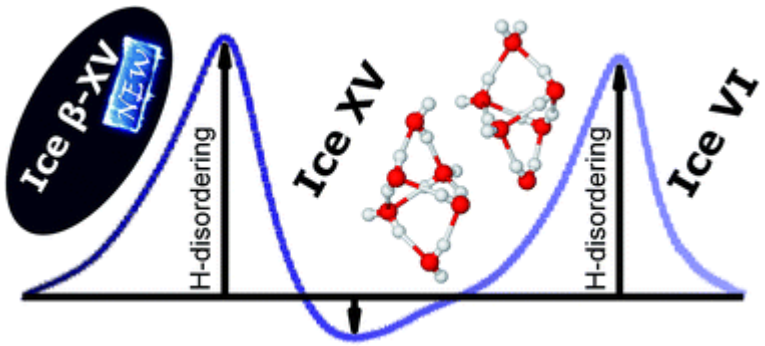

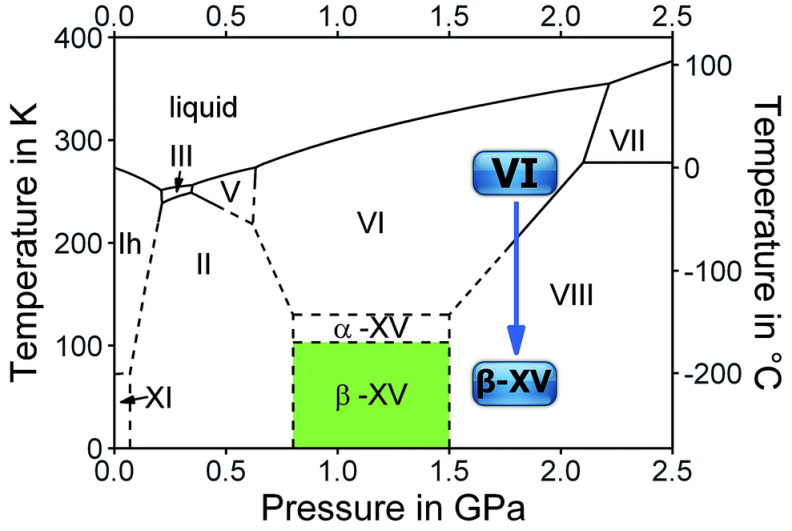

diagram of water. For the time being we suggest to call this new phase ice β-XV and to relabel it ice XVIII once its crystal structure is known.

Characterization tools

❑ Differential scanning calorimetry (DSC)

the difference in the amount of heat required to increase the temperature of a sample and reference is measured as a function of temperature.

Main application: Phase transition

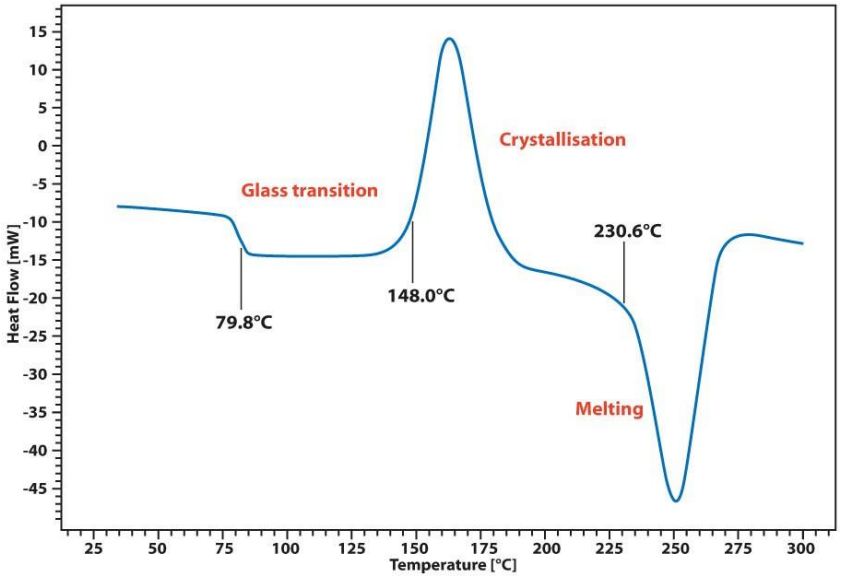

❑ Neutron powder diffraction

the application of neutron scattering is the determination of the atomic and/or magnetic structure of a material.

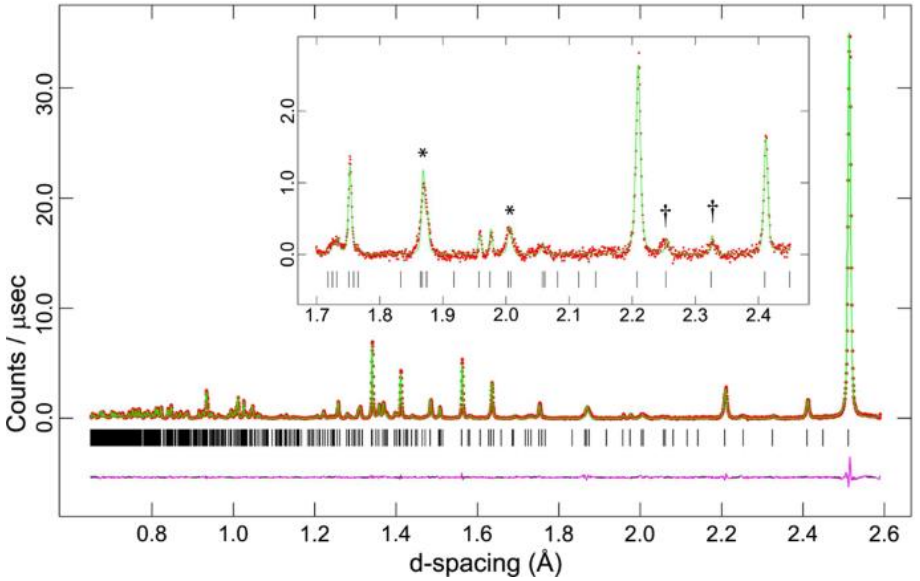

❑ Bernal-Fowler rule/Ice rule:

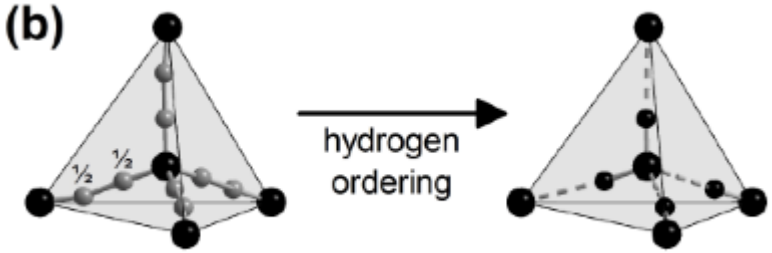

Polymorphs of ice

This unique behavior is due to the geometrical frustration of the weak intermolecular hydrogen bonds and the sizeable quantum motion of the light hydrogen ions.

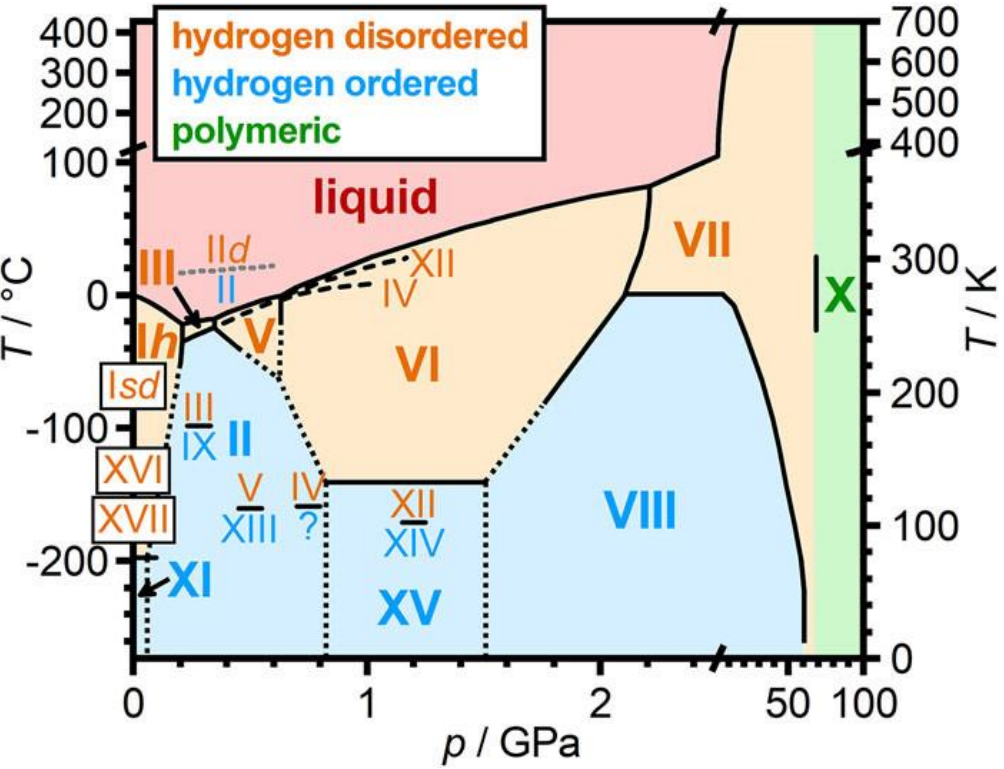

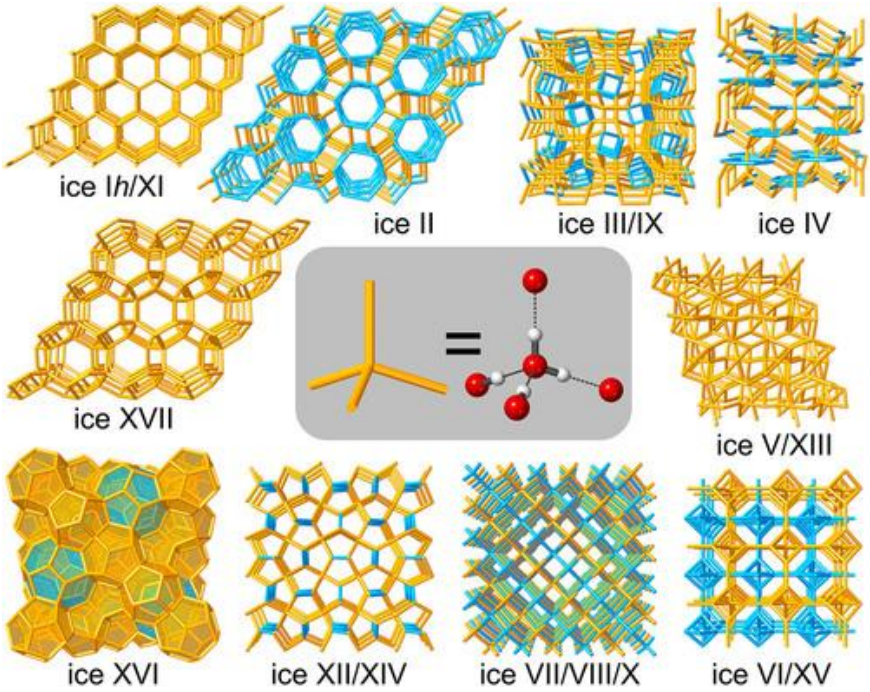

Christoph G. Salzmann; *J. Chem. Phys.* **150,** 060901 (2019)

Acid/base doping of ice and its effect on hydrogen ordering

New ice polymorphs by emptying clathrate hydrates

Background work

Published: 10 December 2014

Formation and properties of ice XVI obtained by emptying a type sII clathrate hydrate

Andrzej Falenty, Thomas C. Hansen & Werner F. Kuhs

Nature **516**, 231–233(2014) | Cite this article

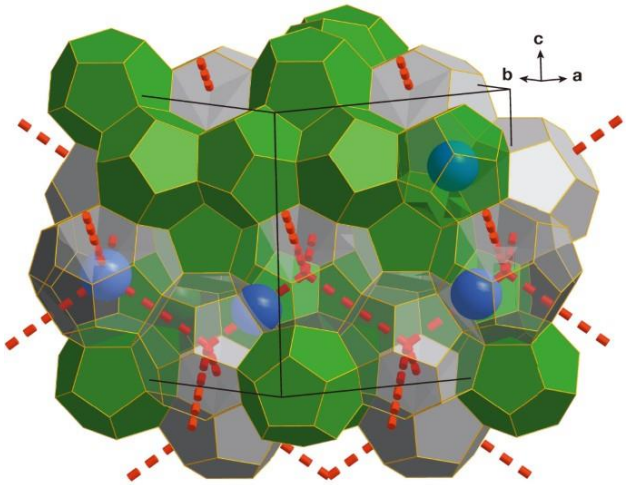

Open Access | Published: 07 November 2016

New porous water ice metastable at atmospheric pressure obtained by emptying a hydrogen-filled ice

Leonardo del Rosso, Milva Celli & Lorenzo Ulivi

Nature Communications **7**, Article number: 13394 (2016) | Cite this article

Letter | Published: 08 May 2019

Nanosecond X-ray diffraction of shock-compressed superionic water ice

Marius Millot, Federica Coppari, J. Ryan Rygg, Antonio Correa Barrios, Sebastien Hamel, Damian C. Swift & Jon H. Eggert

Nature **569**, 251–255(2019) | Cite this article

EDGE ARTICLE

View Article Online
View Journal | View Issue

Cite this: *Chem. Sci.*, 2018, **9**, 4224

Experiments indicating a second hydrogen ordered phase of ice VI

Tobias M. Gasser,[a] Alexander V. Thoeny,[a] Lucie J. Plaga,[b] Karsten W. Köster,[b] Martin Etter,[c] Roland Böhmer[b] and Thomas Loerting*[a]

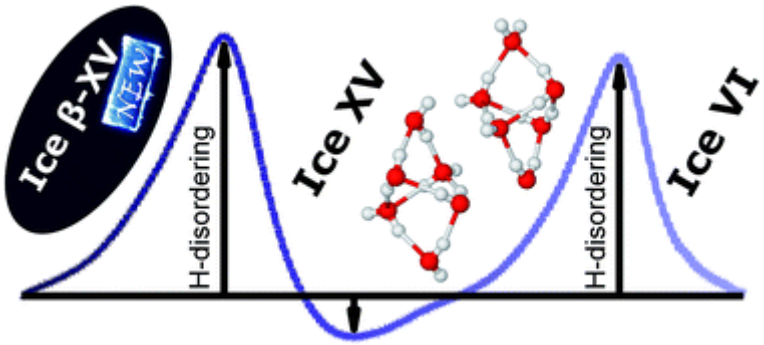

T. M. Gasser, A. V. Thoeny, L. J. Plaga, K. W. Köster, M. Etter, R. Böhmer and T. Loerting, *Chem. Sci.*, 2018, **9**, 4224–4234.

REPORT

The Preparation and Structures of Hydrogen Ordered Phases of Ice

Christoph G. Salzmann[1,2,*], Paolo G. Radaelli[3,4], Andreas Hallbrucker[1], Erwin Mayer[1], John L. Finney[4]

+ See all authors and affiliations

Science 24 Mar 2006:
Vol. 311, Issue 5768, pp. 1758-1761
DOI: 10.1126/science.1123896

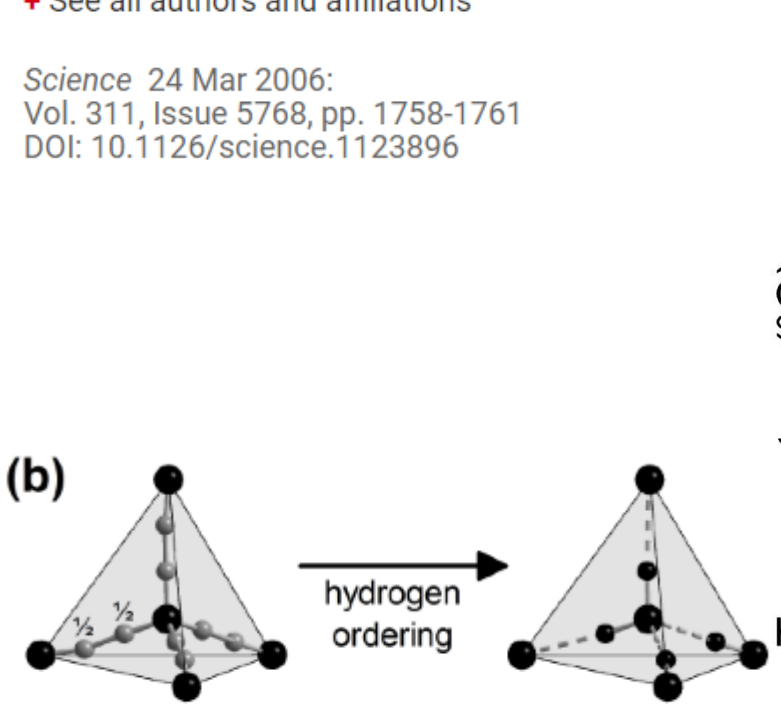

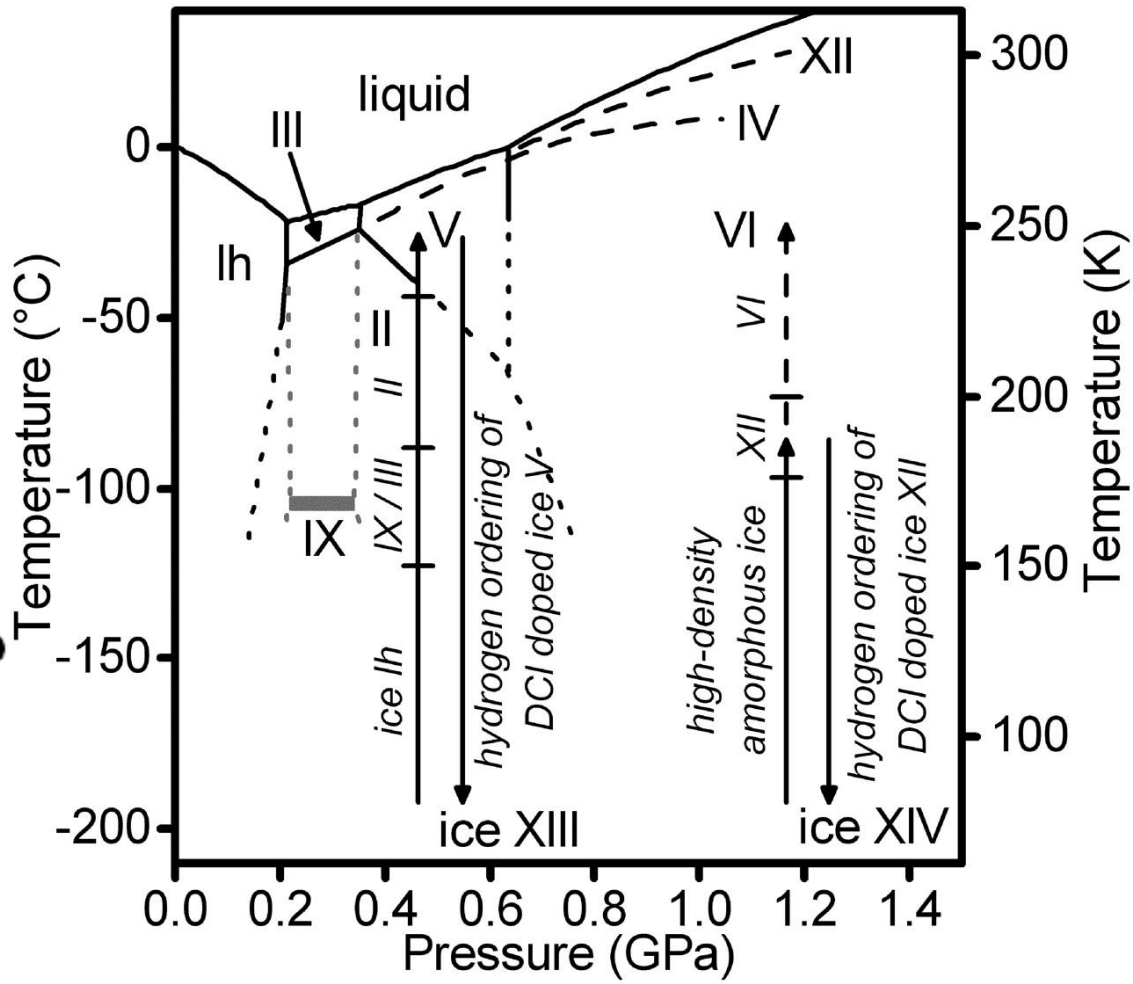

Motivation

(a)

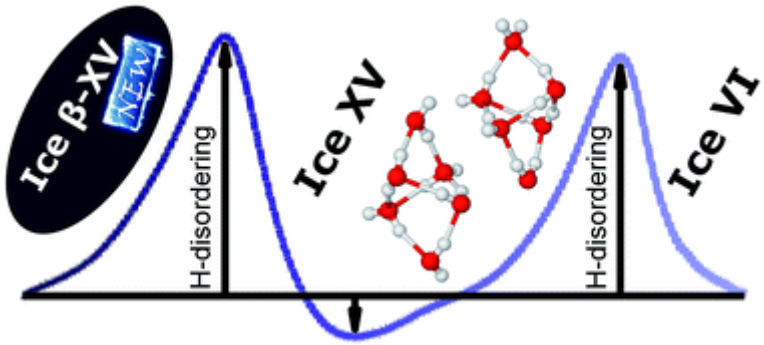

(b)

The slow cooling process that allow
H_2O ice VI → H_2O ice β- XV

just does not allow
D_2O ice VI → D_2O ice β-XV

Introduction

- Disordered ice VI exists in a broad pressure range between 0.6 and 2.2 GPa and at temperatures up to 355 K. It is found naturally in Earth´s mantle and in the interior of icy moons such as the Galilean satellites.

- Partially antiferroelectrically ordered ice XV forms from ice VI upon cooling only in the presence of acid doping (HCl).

- HCl doping introduces an ionic H_3O^+ defect, together with a Bjerrum-L-defect. Such defects are known to accelerate the re-orientational dynamics by up to five orders of magnitude.

- The ordering process to yield ice XV seems to be impeded at high-pressures, but alleviated at ambient pressure.

- In 2018, it was claimed that the ordering process to ice XV is not only slowed down severely near 2 GPa, but instead a transition to a differently-ordered phase takes over. This ordering process leads to a phase called ice β-XV.

- The ice XIX to ice XV transition incurred upon heating represents, to the best of our knowledge, the only order-to-order transition in the H-sublattice known in any kind of water ice.

Experimental procedures:

Ice XIX

(i) Cooling 600 µl 0.01 M DCl in D_2O:H_2O mixtures (0.04 to 99.99% H_2O) to 77 K,

(ii) compressing to 1.8 GPa,

(iii) heating to 255 K, followed

(iv) slow cooling at rates of 0.1 to 3.0 K min^{-1} to 77 K.

Undoped ice VI

(i) 95:5 D_2O:H_2O mixture

(ii) cooling to 77 K,

(iii) compressed to 1.0 GPa,

(iv) heating to 255 K,

(v) quenching with liquid nitrogen at ≈ 80 K min^{-1}.

Ice XV

(i) prepared in situ from ice XIX,

(ii) heating to 135 K at 50 mbar (converting it to ice VI),

(iii) then re-cooling it with 0.4 K min^{-1} to 70 K (converting it to ice XV).

After releasing the pressure at 77 K, ice XIX and ice VI samples were recovered and stored under liquid nitrogen at atmospheric pressure.

Characterization

Differential scanning calorimetry

- All ices were analyzed by Perkin Elmer DSC 8000 at **ambient pressure**.
- Every batch was characterized by heating at **10 K min^{-1}** from **93 to 253 K**.
- **Ice XIX → Ice VI$_{‡}$ → Ice XV → Ice VI → Ice I$_h$**

Neutron powder diffraction

Data were recorded out to 10 Å and used the highest resolution data in the backscattering banks at d-spacings from 0.65 to 2.60 Å for structure refinements.

Refinement of neutron powder data

The data were refined by the Rietveld method in GSAS/Expgui

Results

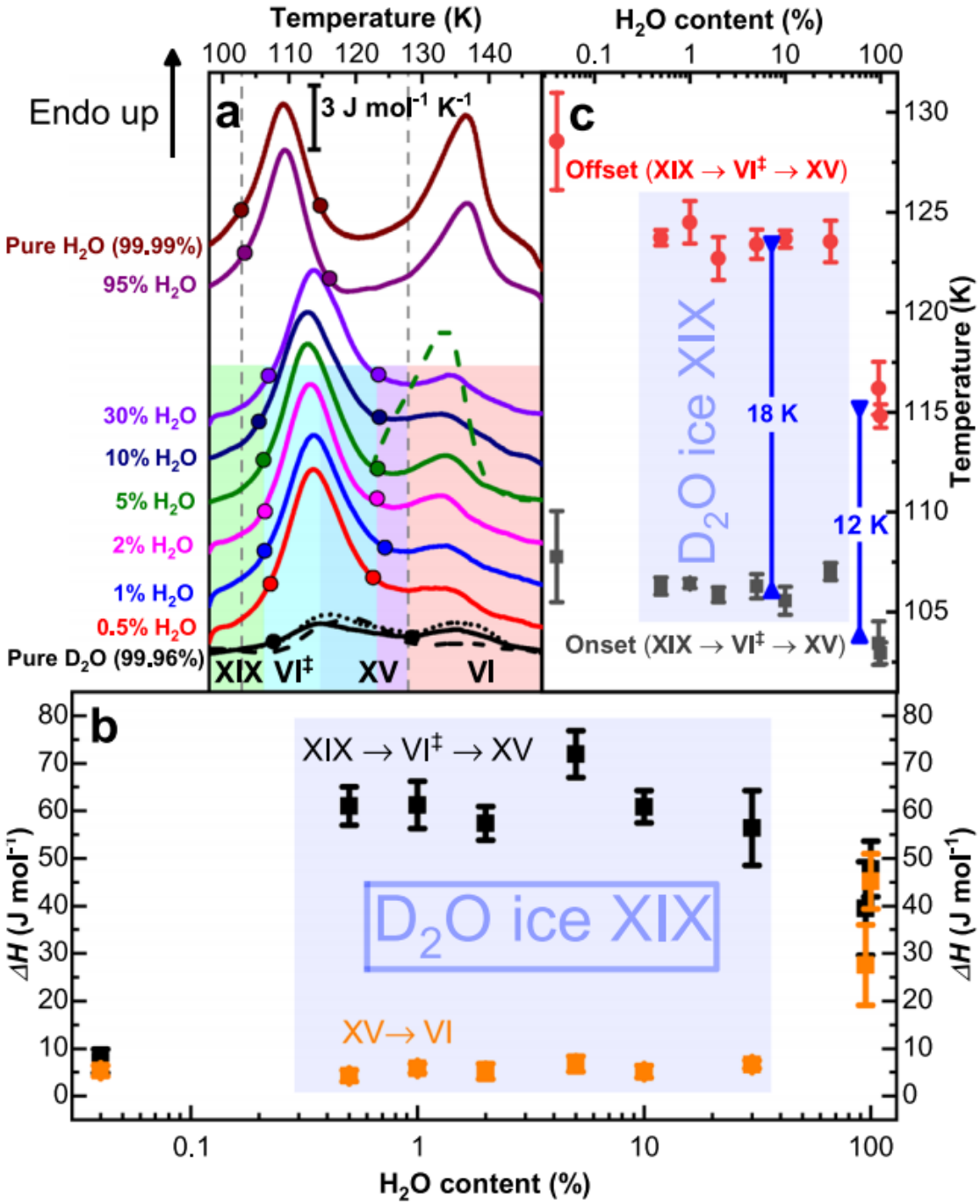

Fig. 1 Calorimetric characterization of hydrogen order. **a** Differential scanning calorimetry traces of ice XIX samples with different D_2O/H_2O ratios recorded at a heating rate of 10 K/min. The two endotherms indicate first the ice XIX → $VI_‡$ → XV and second the ice XV → VI transition. All full lines were recorded on samples slow-cooled at 1.8 GPa (see Methods). Dashed lines mark heating scans of ice XIX annealed at 1.8 GPa and 106 K (black dashed line, pure D_2O) and annealed at ambient pressure and 120 K (green dashed line, 5% H_2O). Heating scan of ice XIX after very slow cooling at 1.8 GPa is shown as dotted black line (pure D_2O). Onset and offset points for the first transition are marked by full circles. **b** Enthalpy changes associated with the two transitions (black squares: XIX → $VI_‡$ → XV; orange squares: XV → VI). **c** Onset (black squares) and offset points (red circles). Error bars in **b** and **c** reflect both reproducibility and ambiguities in determining the points based on the tangent method. The width of the transition at 10 K/min is indicated through the blue double arrow.

Neutron powder diffraction: comparing ice VI, XV and ice XIX.

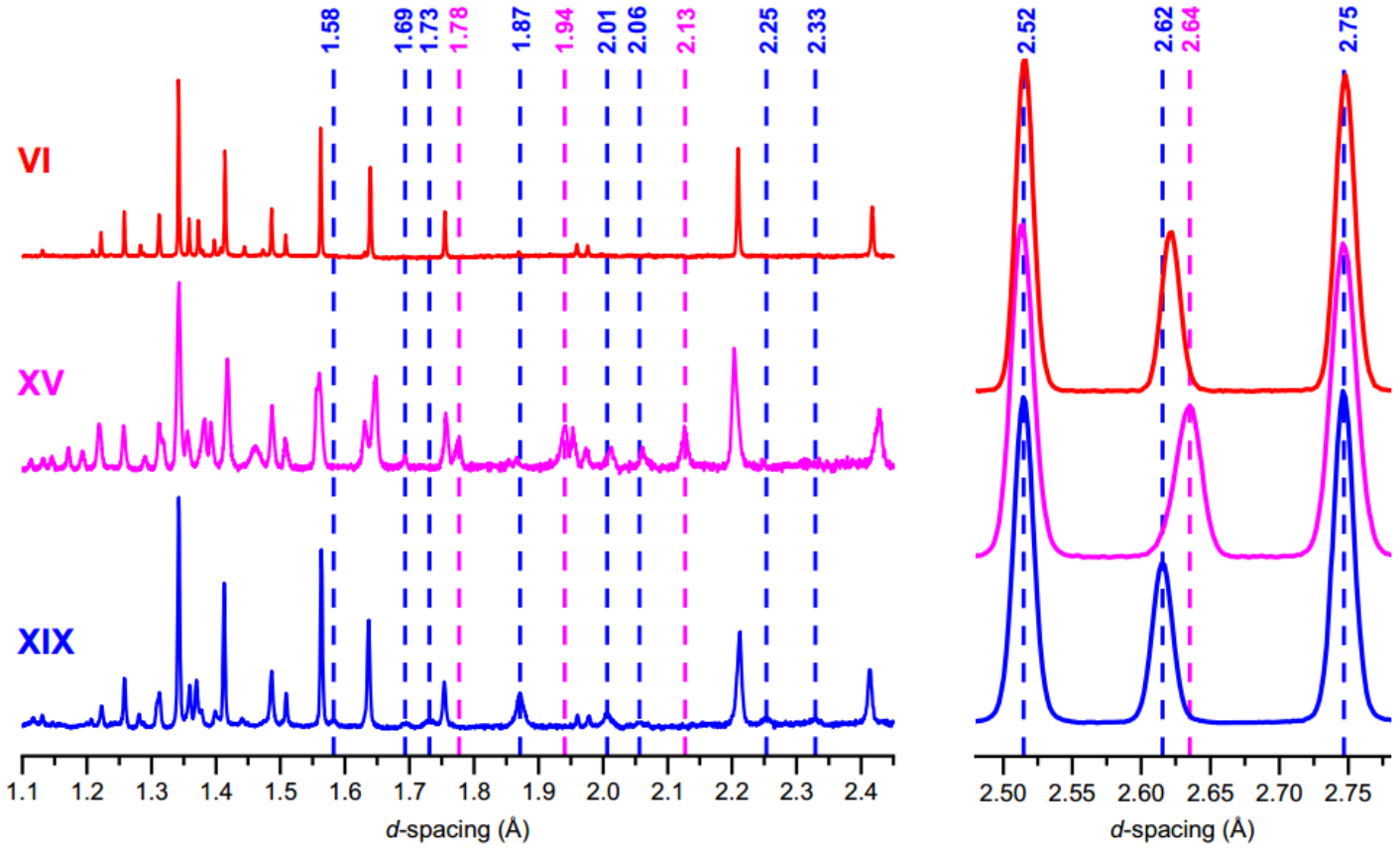

Fig. 2 Comparison of ice XIX, ice XV and ice VI neutron powder diffraction patterns. Baselines were corrected with an 8 pt spline. Selected features of the ice XIX and ice XV diffractograms are highlighted by vertical, dashed blue and magenta lines, respectively. Note the sharp peaks in ice VI and the broader peaks in ices XV and XIX—this hints at particle size broadening originating from very small partially ordered domains. The diffractograms on the left were acquired in the highest resolution backscattering banks ($2\theta = 165 \pm 11°$) whilst the three peaks shown on the right were recorded in the medium resolution detectors at $2\theta = 90 \pm 10°$.

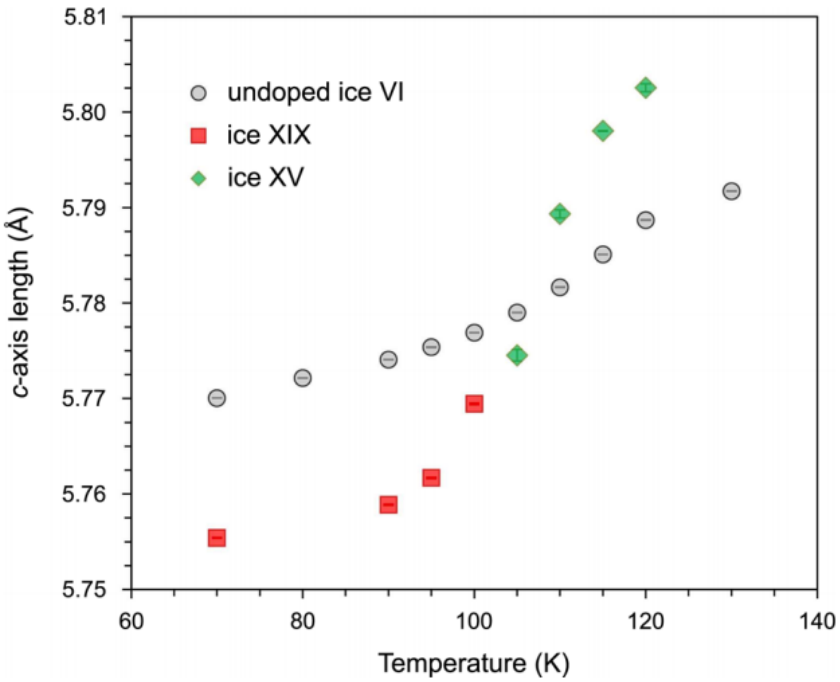

Fig. 4 Unit cell data. Change in the *c*-axis length upon heating ice XIX (red squares and green diamonds, obtained from Rietveld refinement of the data set shown in Fig. 3) compared with a heating scan of undoped ice VI (circles).

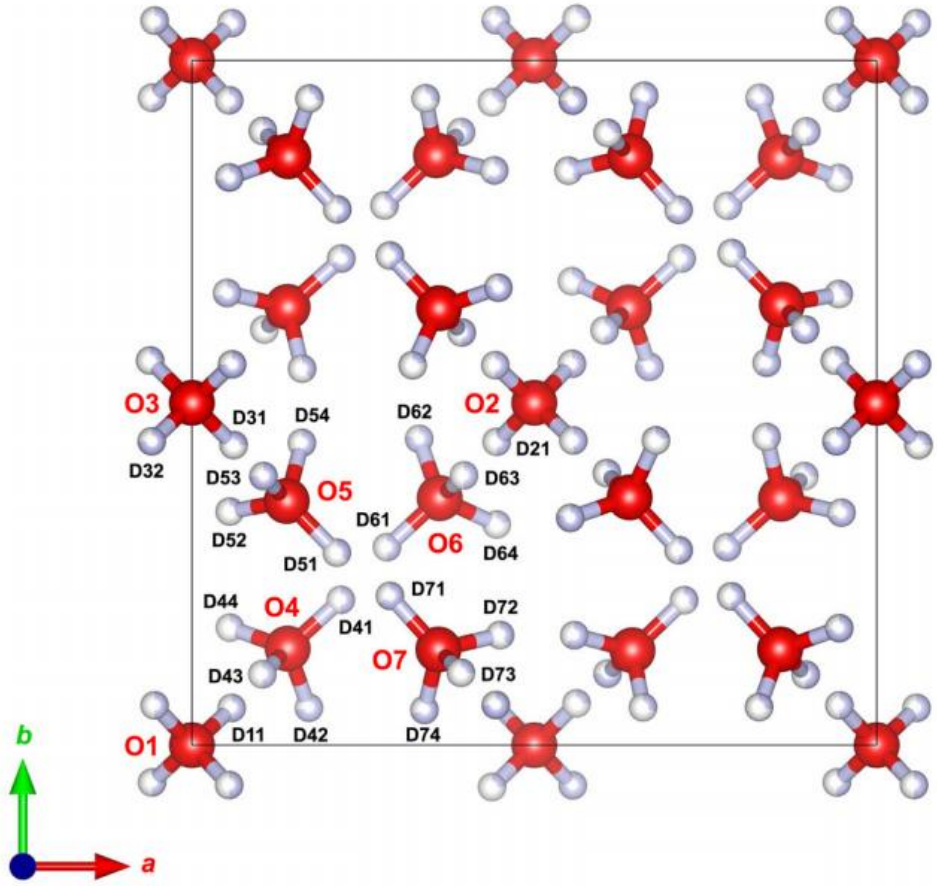

Fig. 6 Unit cell of ice XIX (refined $P\bar{4}$ model). View along the *c*-axis, showing the atom labelling scheme used in Table 1. Shading of the hydrogen atoms indicates the occupancy, reported quantitatively in Table 1.

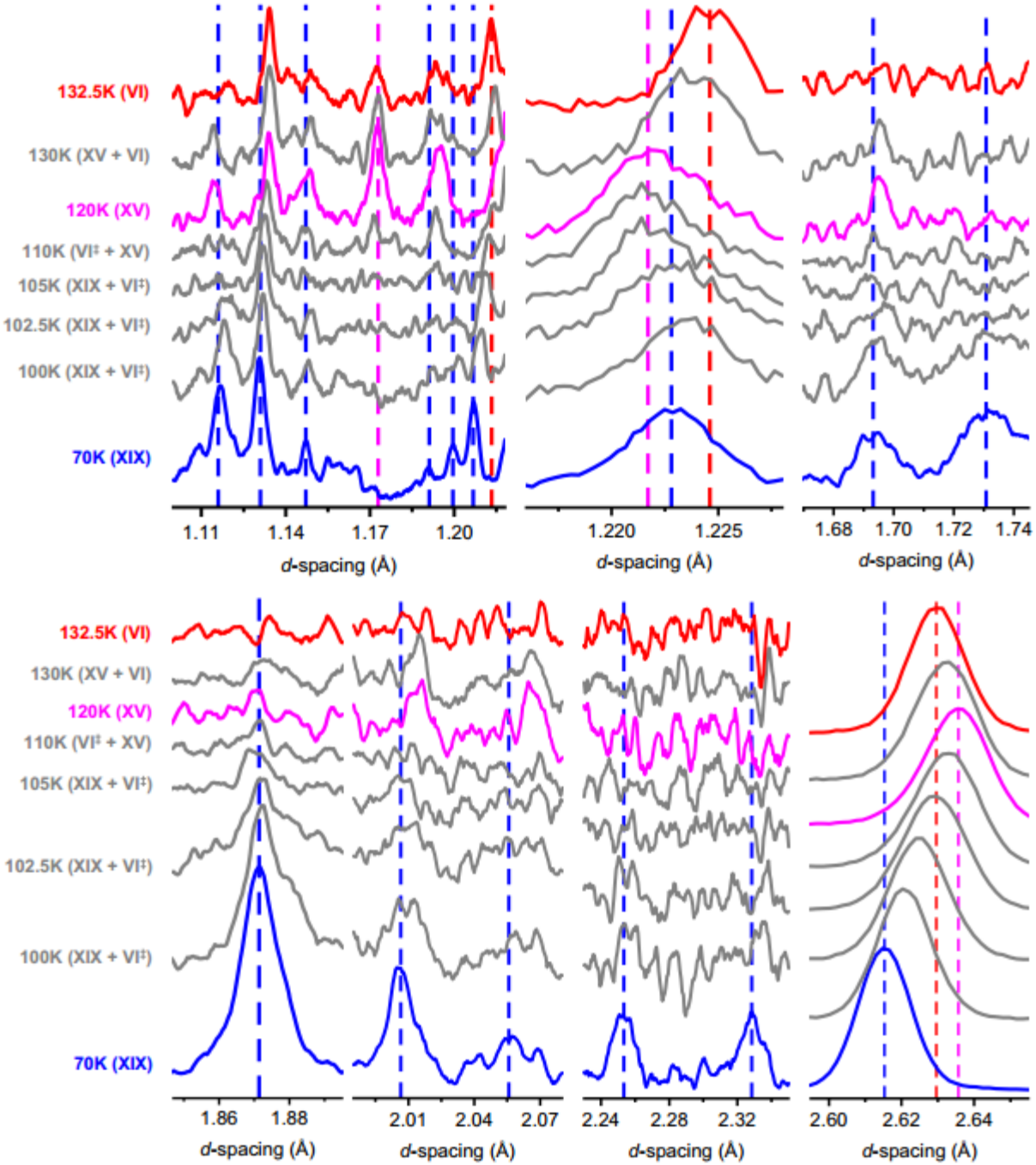

Order-order transition ice XIX → ice XV based on neutron powder diffraction:

Fig. 3 Neutron diffraction of the order-order-disorder transition. Heating of a D2O ice XIX sample in the High Resolution Powder Diffractometer (HRPD), revealing transitions to ice XV (120 K) (via ice VI‡) and to ice VI (132.5 K). Data in panels 1, 3, 4, 5 and 6 were smoothed using a 13 pt Savitzky-Golay. Blue, purple and red dashed lines mark important Bragg peaks for ice XIX, XV and VI, respectively.

Conclusion:

- Ice XIX is slightly better ordered compared to ice XV based on the calorimetry data, where D_2O and H_2O ice XIX release 18% and 14% of the Pauling entropy upon disordering, respectively, compared to 10% in case of H_2O ice XV.

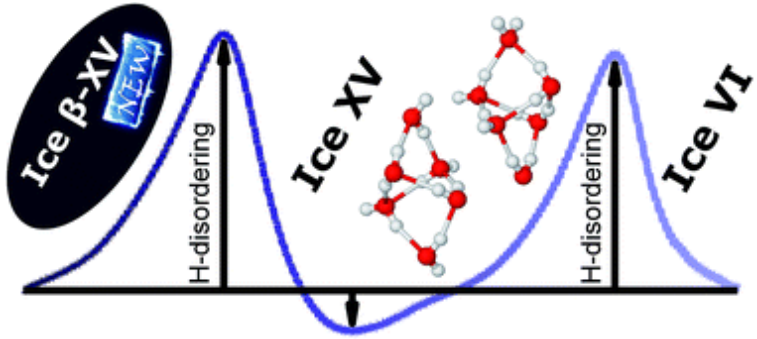

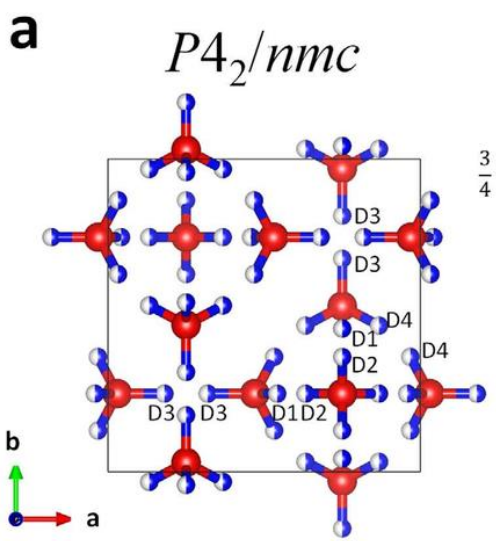

Ice VI

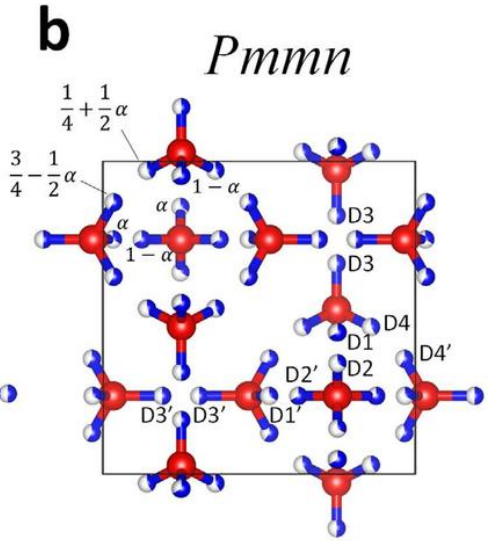

Ice XV

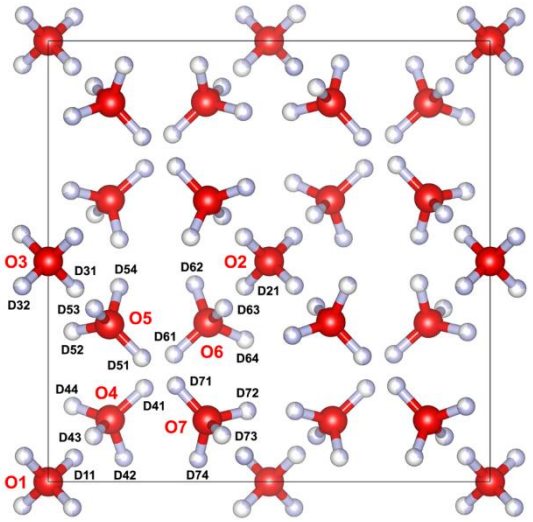

Ice XIX

supercell

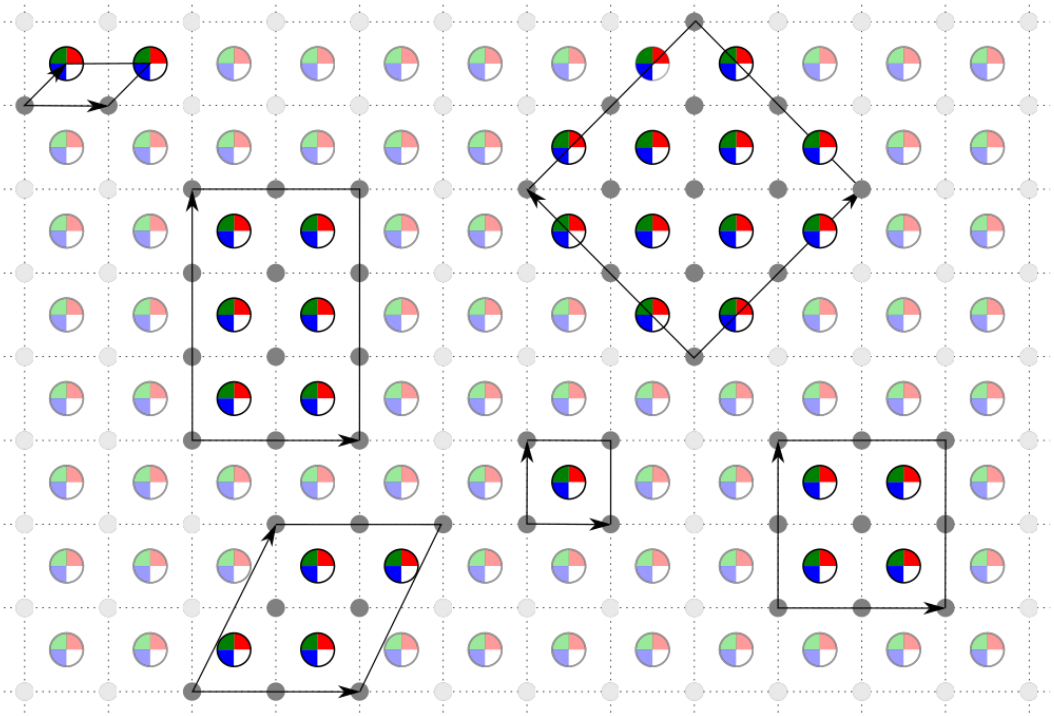

An example of different supercell for 2D cubic crystal. Both diagonal and non-diagonal supercells presented.